








Conjugates of 8-[2,2'-bipyridinyl]coumarins as potential chemosensors for Al³⁺, Cu²⁺, Cd²⁺, Zn²⁺ ions: synthesis and photophysical properties

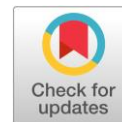
Ainur D. Sharapov ^{a*} , Ramil F. Fatykhov ^a , Igor A. Khalymbadza ^a , Dmitry S. Kopchuk ^{ab} , Igor L. Nikonov ^{abc} , Anastasiya P. Potapova ^a, Yaroslav K. Shtaitz ^a , Pavel A. Slepukhin ^{ab} 

a: Institute of Chemical Engineering, Ural Federal University, Ekaterinburg 620002, Russia

b: I.Ya. Postovsky Institute of Organic Synthesis of Ural Branch of the RAS, Ekaterinburg 620137, Russia

c: Ural State Forest Engineering University, Ekaterinburg 620100, Russia

* Corresponding author: a.d.sharapov@urfu.ru



This paper belongs to a Regular Issue.

Abstract

In this work, we report the synthesis of novel coumarin-bipyridine conjugates using a sequence of C–C coupling reaction between 5,7-dimethoxycoumarins and 3-pyridyl-6-aryl-1,2,4-triazines followed by the Boger reaction with norbornandiene to obtain 8-[2,2'-bipyridyl]-5,7-dimethoxycoumarins. Photophysical properties were investigated for the obtained series of 8-[2,2'-bipyridyl]-5,7-dimethoxycoumarins: absorption and emission wavelength maxima are in the region of 212–296 and 401–410 nm, respectively; Stokes shifts are up to 116 nm, and fluorescence quantum yields are up to 15.0%. It was found that titrating the conjugates with Al³⁺, Zn²⁺, and Cd²⁺ ions results in an increase in the intensity of the emission maxima of the complexes, while the opposite effect was observed in the case of titration with Cu²⁺ ions. These findings suggest that the studied compounds may be considered as promising chemosensing materials. Finally, a positive solvatochromism of 8-[2,2'-bipyridyl]coumarins and their metal complexes was established. The experimental data are supported by mathematical calculations according to the Lippert-Mataga equation and Kosower diagram.

Keywords

chemosensors
coumarins
2,2'-bipyridines
photophysical properties
metal complexes

Key findings

- A new series of 8-[2,2'-bipyridyl]-5,7-dimethoxycoumarins with good yields and high regioselectivity was prepared.
- The obtained compound are characterized by λ_{abs} and λ_{em} in the range of 212–296 and 401–410 nm, respectively, $\Delta\lambda$ up to 116 nm, and quantum yields up to 15.0%.
- 8-[2,2'-bipyridinyl]coumarins demonstrate promising chemosensing properties towards Al³⁺, Cu²⁺, Cd²⁺, Zn²⁺ ions.

Received: 14.11.23

Revised: 19.11.23

Accepted: 19.12.23

Available online: 28.12.23

© 2023, the Authors. This article is published in open access under the terms and conditions of the Creative Commons Attribution (CC BY) license (<http://creativecommons.org/licenses/by/4.0/>).



1. Introduction

The coumarin is a promising scaffold for the preparation of a wide range of materials with valuable properties. Although unsubstituted coumarin has low fluorescence in the visible light [1], many properly substituted coumarin derivatives show fluorescence in a wide range [2–5]. Moreover, coumarins are widely used as fluorescent chemosensors for various analytes, including inorganic anions [6–11], metal cations [12–16], reactive oxygen species [17, 18], sulfur [19, 20] or nitrogen [21–23], and biologically active compounds [24, 25].

A variety of substituted coumarins as chemosensors, which are basically “push-pull” systems, are commercially available compounds (Figure 1) [26].

It is known that many coumarins as chemosensors interact with ions Al³⁺, Cu²⁺, Cd²⁺, Zn²⁺ by coordination mechanism (Scheme 1).

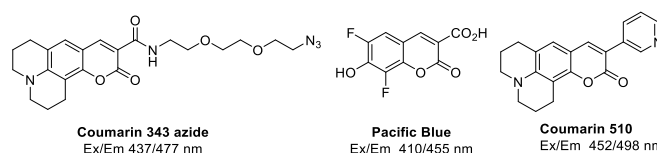
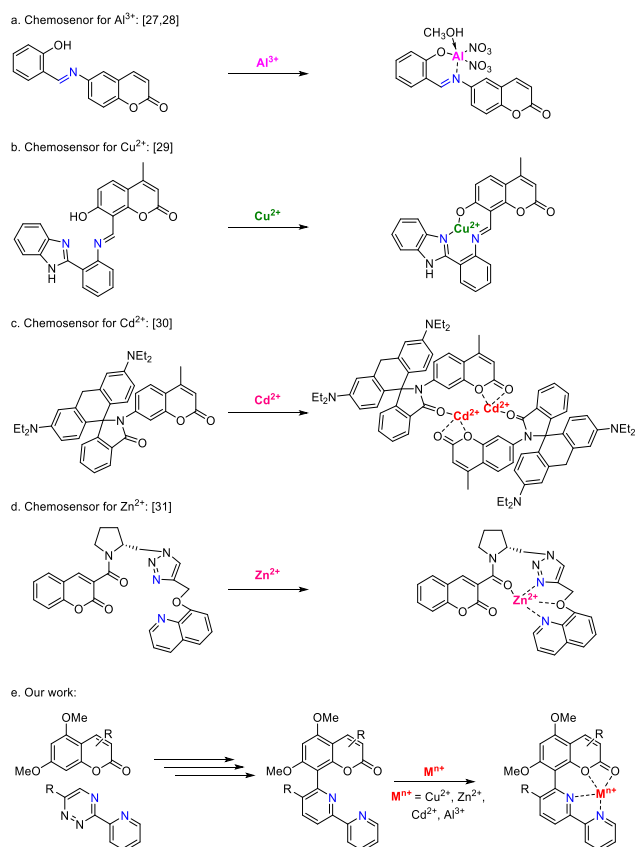


Figure 1 Some commercially available fluorescent coumarins.

For example, many coumarin-based sensors are known for aluminum cations, which are able to "turn on" fluorescence with the formation of a stable complex, as well as with the inhibition of the PET effect [27, 28] (Scheme 1a). In the case of interaction of fluorophores with copper ions, the mechanism of fluorescence quenching at coordination with Cu^{2+} by the PET mechanism is realized [29] (Scheme 1b). Dey's group developed a coumarin-rhodamine FRET-sensor for the determination of Cd^{2+} ions. In aqueous methanol solution, the probe showed a 19-fold fluorescence enhancement in the operating range of pH = 6–10 (Scheme 1c) [30]. Govindaraju's group reported a triazole-containing ligand (Scheme 1d), which showed fluorescence response to several metal ions in aqueous solution containing a small amount of acetonitrile. In the case of determination of zinc ions, Zn^{2+} fluorescence enhancement at 418 nm was observed [31].

In our presented work, we obtained bipyridine-coumarin conjugates, which showed fluorescence response to Al^{3+} , Cu^{2+} , Cd^{2+} , and Zn^{2+} ions, for which the photophysical properties and the influence of solvent polarity were studied.

Previously, we carried out nucleophilic hydrogen substitution reactions, which showed great efficiency in the synthesis of monoazinyl derivatives of coumarins and conjugates based on monopyridine coumarins [32–34]. This strategy was also applied to the synthesis of bipyridine-coumarin conjugates, and the efficiency was confirmed by good yields and high selectivity.



Scheme 1 Chemosensors based on coumarin framework.

Thus, in the present work, we further developed this synthetic protocol for bipyridine-coumarins conjugates and studied the photophysical properties to obtain potential chemosensors for metal ions such as Cd^{2+} , Cu^{2+} , Zn^{2+} , Al^{3+} .

2. Experimental

2.1. Materials and equipment

NMR spectra were recorded on a Bruker Avance-400 spectrometer, 298 K, digital resolution ± 0.01 ppm. Chemical shifts are expressed in ppm (δ) and refer to residual signals of solvent, and signals are designated as *s* (singlet), *d* (doublet), *t* (triplet), *m* (multiplet); coupling constants *J* are given in Hz. TMS (tetramethylsilane) was used as an internal standard (for ^1H and ^{13}C). Thin layer chromatography (TLC) was performed on silica gel coated glass slide (Merck, Silica Gel G for TLC). Silica gel (60–120 mesh, SRL, India) was used for column chromatography. Microanalysis (C, H, N) was carried out on a Perkin–Elmer 2400 elemental analyzer. All solvents were dried and distilled before use. All reactions involving moisture-sensitive reagents were performed using oven-dried glassware. Fluorescence spectra were measured on a Horiba-Fluoromax-4 spectrofluorimeter. UV/Vis absorption spectra were recorded using a Shimadzu UV-2550 UV-Vis spectrometer.

The starting coumarins were obtained according to the procedure described in [35, 50]. Triazines were obtained according to methods known in the literature [32–34, 36].

The XRD experiment was accomplished on equipment of the 'SAOC' centre of collective using IOS UB RAS using the automated 'Xcalibur 3' diffractometer with the standard procedure (Mo K-irradiation, graphite monochromator, ω -scans with 1° step). Empirical absorption correction was applied. The collection, data reductions and refinement of the unit cell parameters were carried out using the CrysAlisPro program. The structures were solved with the ShelXS structure solution program using direct method and refined with the ShelXL refinement program using Least Squares minimization in anisotropic approximation for nonhydrogen atoms [48, 49].

2.2. General procedure for the synthesis of coumarin-triazines conjugates 3a-d

To a dichloromethane solution of the corresponding coumarin (1 eq.) **1a–d**, corresponding 1,2,4-triazine **2a, b** and methanesulfonic acid (10 eq. 960 mg) was added, and the mixture was stirred at room temperature for 12 hours. After completion of the reaction, the dichloromethane was distilled off from the reaction mixture, and the residue was neutralized to pH = 7. Then, DDQ (2,3-dichloro-5,6-dicyano-1,4-benzoquinone) (1.1 eq.) or chloranil (1.2 eq.) in 1,2-dichloroethane (10 ml) was added, and the mixture was heated at 80 °C. The pure products **3a–d** were isolated using silica gel flash chromatography (hexane:ethyl acetate = 1:1).

2.2.1. 5-(5,7-Dimethoxy-4-phenyl-2H-chromen-2-on-8-yl)-3-(pyridyl-2)-6-tolyl-1,2,4-triazine (3a)

Yield 70%. Light orange powder, m.p. 283–285 °C. ¹H NMR (CDCl₃, δ, ppm): 2.34 (s, 3H, Me), 3.46 (s, 3H, OMe), 3.56 (s, 3H, OMe), 5.97 (s, 1H, H³), 6.15 (s, 1H, H⁶), 7.14 (d, ¹J = 7.8 Hz, 1H, H_o), 7.25 (s, 2H, H_o), 7.41–7.34 (m, 3H, H_{m+p}), 7.5–7.46 (m, 3H, H_o, H⁵(Py)), 7.96 (t, ¹J = 7.5 Hz, 1H, H⁴(Py)), 8.76 (d, ¹J = 7.9 Hz, 1H, H³(Py)), 8.92 (d, ¹J = 4.0 Hz, 1H, H⁶(Py)). ¹³C NMR (CDCl₃, δ, ppm): 21.5, 55.7, 56.1, 91.4, 103.8, 107.6, 113.5, 124.5, 125.6, 127.1, 127.6, 128.2, 128.5, 129.1, 132.6, 137.7, 139.7, 139.8, 150.1, 152.7, 152.8, 153.4, 153.8, 154.3, 155.3, 159.5, 159.7, 159.8, 160.5, 161.1. Found, %: C 72.65, H 4.32, N 10.78. C₃₂H₂₄N₄O₄. Calcd., %: C 72.72, H 4.58, N 10.60.

2.2.2. 5-(5,7-Dimethoxy-4-methyl-2H-chromen-2-on-8-yl)-3-(pyridyl-2)-6-phenyl-1,2,4-triazine (3b)

Yield 54%. Light orange powder, m.p. 272–274 °C. ¹H NMR (CDCl₃, δ, ppm): 2.50 (s, 3H, Me), 3.55 (s, 3H, OMe), 3.88 (s, 3H, OMe), 5.89 (s, 1H, H³), 6.22 (s, 1H, H⁶), 7.38–7.25 (m, 3H, H_{m+p}), 7.45–7.38 (m, 1H, H⁵(Py)), 7.53 (d, ¹J = 6.8 Hz, 2H, H_o), 7.93–7.85 (m, 1H, H⁴(Py)), 8.70 (d, ¹J = 7.9 Hz, 1H, H³(Py)), 8.86 (d, ¹J = 4.1 Hz, 1H, H⁶(Py)). ¹³C NMR (CDCl₃, δ, ppm): 24.5, 55.9, 56.0, 91.0, 104.9, 107.2, 112.1, 124.4, 125.3, 128.2, 128.5, 129.5, 135.5, 137.1, 150.5, 153.0, 153.1, 154.0, 154.2, 159.4, 159.8, 159.9, 160.7, 161.7. Found, %: C 69.26, H 4.22, N 12.51. C₂₆H₂₀N₄O₄. Calcd., %: C 69.02, H 4.46, N 12.38.

2.2.3. 5-(5,7-Dimethoxy-4-methyl-2H-chromen-2-on-8-yl)-3-(pyridyl-2)-6-tolyl-1,2,4-triazine (3c)

Yield 58%. Light orange powder, m.p. 262–264 °C. ¹H NMR (CDCl₃, δ, ppm): 2.31 (s, 3H, Me), 2.52 (s, 3H, Me), 3.58 (s, 3H, OMe), 3.90 (s, 3H, OMe), 5.90 (s, 1H, H₃), 6.24 (s, 1H, H₆), 7.09 (d, ¹J = 7.9 Hz, 2H, H_m), 7.41 (d, ¹J = 5.4 Hz, 1H, H₅(Py)), 7.44 (d, ¹J = 7.9 Hz, 2H, H_o), 7.89 (td, ¹J = 7.5 Hz, ²J = 1.3 Hz, 2H, H₄(Py)), 8.70 (d, ¹J = 7.9 Hz, 1H, H₃(Py)), 8.86 (d, ¹J = 4.4 Hz, 1H, H₆(Py)). ¹³C NMR (CDCl₃, δ, ppm): 21.5, 24.5, 56.0, 56.1, 91.0, 104.9, 107.5, 112.2, 124.4, 125.3, 128.5, 129.0, 132.6, 137.1, 139.6, 150.5, 152.9, 153.2, 154.0, 154.2, 159.4, 159.9, 160.0, 160.6, 161.5. Found, %: C 71.71, H 4.82, N 11.58. C₂₇H₂₂N₄O₄. Calcd., %: C 71.52, H 4.75, N 12.01.

2.2.4. 5-(5,7-Dimethoxy-3-benzyl-4-methyl-2H-chromen-2-on-8-yl)-3-(pyridyl-2)-6-tolyl-1,2,4-triazine (3d)

Yield 67%. Light orange powder, m.p. 221–223 °C. ¹H NMR (CDCl₃, δ, ppm): 2.32 (s, 3H, Me), 3.58 (s, 3H, OMe), 2.53 (s, 3H, Me), 3.97 (s, 2H, CH₂), 3.89 (s, 3H, OMe), 6.24 (s, 1H, H⁶), 7.10 (d, ¹J = 7.9 Hz, 2H, H_m), 7.20–7.13 (m, 2H, H_o), 7.30–7.21 (m, 3H, H_{m+p}), 7.49–7.37 (m, 3H, H_o, H⁵(Py)), 7.90 (t, ¹J = 7.7 Hz, 1H, H⁴(Py)), 8.70 (d, ¹J = 7.9 Hz, 1H, H³(Py)), 8.86 (d, ¹J = 3.7 Hz, 1H, H⁶(Py)). ¹³C NMR (CDCl₃, δ, ppm): 20.2, 21.5, 32.7, 56.0, 56.1, 91.3, 105.6, 107.2, 121.7, 124.4, 125.3, 126.2, 128.3, 128.5, 128.6, 129.0, 132.7, 137.1, 139.4, 139.5, 149.5, 150.5, 152.7, 153.0, 153.2,

159.2, 159.5, 160.4, 161.0, 161.5. Found, %: C 73.36, H 4.78, N 9.98. C₃₄H₂₆N₄O₄. Calcd., %: C 73.65, H 4.69, N 10.11.

2.2.5. General procedure for the synthesis of coumarin-bipyridine conjugates 4a–d

The corresponding 1,2,4-triazine **3a–d** (0.15 mmol) was suspended in 1,2-dichlorobenzene (15 mL); then, 2,5-norbornadiene (69 μL, 0.75 mmol) was added, and the resulting mixture was stirred at 215 °C in an autoclave in argon atmosphere for 20 h. The solvent was removed under reduced pressure, and the residue was purified by flash chromatography (mixture of DCM and ethyl acetate (10:1) as eluent to obtain pure **4a–d**). The analytical sample was obtained by recrystallization (acetonitrile).

2.2.6. 5,7-Dimethoxy-4-phenyl-8-(5-p-tolyl-2,2'-bipyridin-6-yl)-2H-chromen-2-one (4a)

Yield 73%. ¹H NMR (CDCl₃, δ, ppm): 2.30 (s, 3H, CH₃), 3.43 (s, 3H, OCH₃), 3.60 (s, 3H, OCH₃), 5.95 (s, 1H, H³(coumarine)), 6.14 (s, 1H, H⁶(coumarine)), 7.00–7.05 (m, 2H, C₆H₄CH₃), 7.12–7.16 (m, 2H, C₆H₄CH₃), 7.23–7.30 (m, 3H, Ph), 7.34–7.40 (m, 3H, Ph+H⁵(Py)), 7.73–7.79 (m, 1H, H³(Py)), 7.86 (d, 1H, ³J 8.0 Hz, H³(Py)), 8.38–8.44 (m, 2H, H⁴(Py)+H⁴(Py)), 8.67–8.70 (m, 1H, H⁶(Py)). ¹³C NMR (CDCl₃, δ, ppm): 21.2, 55.5, 55.9, 91.7, 103.6, 112.1, 113.0, 120.5, 122.0, 123.5, 127.5, 127.9, 128.4, 128.6, 129.8, 133.9, 136.9, 138.3, 139.2, 140.2, 149.1, 149.8, 154.2, 155.1, 155.4, 156.5, 158.4, 160.6, 160.7, 165.4. Mass spectrum, *m/z* (*I*_{rel}, %): Found, 527.1979 (100), Calcd., 527.1978 (100) [*M* + *H*]⁺. Found, %: C 77.56, H 4.99, N 5.31. C₃₄H₂₆N₂O₄. Calcd., %: C 77.55, H 4.98, N 5.32.

2.2.7. 5,7-Dimethoxy-4-methyl-8-(5-phenyl-2,2'-bipyridin-6-yl)-2H-chromen-2-one (4b)

Yield 75%. ¹H NMR (CDCl₃, δ, ppm): 2.54 (s, 3H, CH₃), 3.64 (s, 3H, OCH₃), 3.90 (s, 3H, OCH₃), 5.94 (s, 1H, H³(coumarine)), 6.26 (s, 1H, H⁶(coumarine)), 7.21–7.29 (m, 4H, Ph+H⁵(Py)), 7.30–7.35 (m, 2H, Ph), 7.76–7.82 (m, 1H, H³(Py)), 7.91 (d, 1H, ³J 8.0 Hz, H³(Py)), 8.42–8.49 (m, 2H, H⁴(Py)+H⁴(Py)), 8.71–8.75 (m, 1H, H⁶(Py)). ¹³C NMR (CDCl₃, δ, ppm): 24.4, 55.7, 55.8, 76.8, 77.1, 77.4, 91.1, 104.7, 111.5, 111.6, 120.3, 121.9, 123.5, 127.2, 127.8, 128.5, 136.8, 138.2, 139.1, 139.8, 149.0, 149.9, 154.0, 154.1, 155.1, 159.2, 160.1, 160.7. Mass spectrum, *m/z* (*I*_{rel}, %): Found, 451.1653 (100), Calcd., 451.1652 (100) [*M* + *H*]⁺. Found, %: C 74.66, H 4.91, N 6.23. C₂₈H₂₂N₂O₄. Calcd., %: C 74.65, H 4.92, N 6.22.

2.2.8. 5,7-Dimethoxy-4-methyl-8-(5-p-tolyl-2,2'-bipyridin-6-yl)-2H-chromen-2-one (4c)

Yield 75%. ¹H NMR (CDCl₃, δ, ppm): 2.26 (s, 3H, CH₃), 2.52 (s, 3H, CH₃), 3.61 (s, 3H, OCH₃), 3.87 (s, 3H, OCH₃), 3.97–3.99 (m, 2H, CH₂), 5.88 (s, 1H, H³(coumarine)), 6.21 (s, 1H, H⁶(coumarine)), 6.96–7.01 (m, 2H, C₆H₄CH₃), 7.07–7.12 (m, 2H, C₆H₄CH₃), 7.23–7.27 (m, 1H, H⁵(Py)), 7.70–7.75 (m, 1H, H³(Py)), 7.82 (d, 1H, ³J 8.0 Hz, H³(Py)), 8.34–8.41 (m, 2H, H⁴(Py)+H⁴(Py)), 8.65–8.69 (m, 1H, H⁶(Py)). ¹³C NMR (CDCl₃, δ, ppm): 21.1, 24.4, 55.7, 55.8,

91.1, 111.7, 120.2, 121.9, 123.3, 128.3, 128.5, 129.8, 133.8, 136.6, 136.7, 136.8, 138.2, 139.1, 149.0, 149.8, 153.9, 154.9, 156.5, 159.1, 160.1, 160.7, 165.3. Mass spectrum, m/z (I_{rel} , %): Found, 465.1818 (100), Calcd., 465.1817 (100) [$M + H$] $^+$. Found, %: C 75.96, H 5.22, N 6.04. $C_{29}H_{24}N_2O_4$. Calcd., %: C 74.98, H 5.21, N 6.03.

2.2.9. 3-Benzyl-5,7-dimethoxy-4-methyl-8-(5-*p*-tolyl-2,2'-bipyridin-6-yl)-2*H*-chromen-2-one (4d)

Yield 69%. 1H NMR ($CDCl_3$, δ , ppm): 2.27 (s, 3H, CH_3), 2.51 (s, 3H, CH_3), 3.62 (s, 3H, OCH_3), 3.85 (s, 3H, OCH_3), 3.97–3.99 (m, 2H, CH_2), 6.24 (s, 1H, H^6 (coumarine)), 6.97–7.01 (m, 2H, $C_6H_4CH_3$), 7.08–7.12 (m, 2H, $C_6H_4CH_3$), 7.15–7.20 (m, 3H, Ph), 7.22–7.28 (m, 3H, Ph+ $H^{5'}$ (Py)), 7.71–7.77 (m, 1H, $H^{3'}$ (Py)), 7.84 (d, 1H, 3J 8.0 Hz, H^3 (Py)), 8.36–8.43 (m, 2H, H^4 (Py)+ $H^{4'}$ (Py)), 8.66–8.70 (m, 1H, $H^{6'}$ (Py)). ^{13}C NMR ($CDCl_3$, δ , ppm): 20.0, 21.2, 32.6, 55.7, 55.8, 91.5, 105.3, 114.5, 120.2, 121.0, 121.9, 123.3, 126.0, 128.2, 128.4, 129.8, 133.8, 136.6, 136.8, 136.9, 139.2, 139.7, 149.0, 149.5, 149.9, 152.4, 154.9, 156.5, 158.9, 159.3, 161.5, 165.3. Mass spectrum, m/z (I_{rel} , %): Found, 555.2293 (100), Calcd., 555.2292 (100) [$M + H$] $^+$. Found, %: C 77.95, H 5.47, N 5.04. $C_{36}H_{30}N_2O_4$. Calcd., %: C 77.96, H 5.45, N 5.05.

2.2.10. Crystal data for 4b

$C_{28}H_{22}N_2O_4$ ($M = 450.47$), monoclinic, space group $P2_1/c$ at 295(2) K: $a = 7.2510(9)$, $b = 16.3628(17)$ and $c = 19.364(2)$ Å, $\beta = 96.566(13)^\circ$, $V = 2282.4(5)$ Å 3 , $Z = 4$, $d_{calc} = 1.311$ g·cm $^{-3}$, $\mu(Mo K\alpha) = 0.088$ mm $^{-1}$, $F(000) = 944$. On the angles $7.118^\circ \leq 2\theta \leq 52.73^\circ$ total of 12889 reflections were collected (4614 independent reflections, $R_{int} = 0.0909$, $R_{sigma} = 0.1273$) which were used in all calculations. The final $R_1 = 0.0615$, $wR_2 = 0.1141$ [for reflections with $I > 2s(I)$] and $R_1 = 0.1757$, $wR_2 = 0.1649$ (for all data), $GOOF = 0.944$. Largest diff. peak and hole 0.16/−0.21 eÅ $^{-3}$.

3. Result and Discussion

3.1. Synthesis

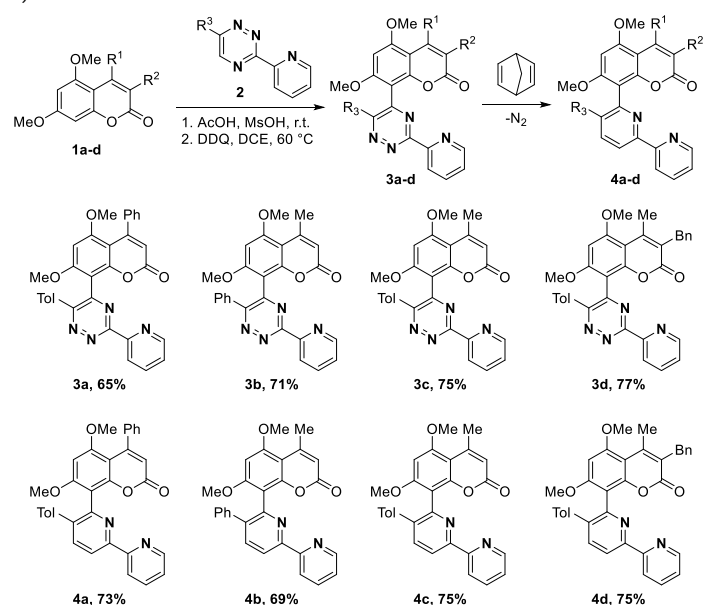
We have recently described the synthesis of 8-(2,5-diaryl)pyridylcoumarins and evaluated their photophysical properties [34]. The results of photophysical studies revealed a number of advantages of the combined pyridine-coumarin fluorophore systems over both coumarins and diarylpyridines, including the previously published 2,5-diarylpyridines with an alkoxy group at the C-6 position. Positive solvatochromia was demonstrated for the two most representative fluorophores, and the data were analyzed using the Lippert-Mataga equation as well as the Kosower and Dimroth/Reichardt scales.

In this report, we wish to expand the scope of this method by exemplifying the synthesis of 8-[2,2'-bipyridinyl]coumarins **4a–d** as well as studying their photophysical properties and evaluating them as potential chemosensors for Al^{3+} , Cu^{2+} , Cd^{2+} , and Zn^{2+} ions. The synthetic route to 8-[2,2'-bipyridinyl]coumarins is shown in Scheme 2.

At the beginning of this work, starting triazines **2** were obtained according to the optimized synthetic approach [32, 33, 34, 36] using the reaction of interaction of amidrazones with glyoxal. In particular, the reaction was carried out in a chloroform:water mixture at 60 °C for 2 days to increase the yield.

The subsequent C-C coupling of 5,7-dimethoxycoumarins **1a–d** with 1,2,4-triazines **2a, b** was carried out by nucleophilic addition at the C-5 position of the 1,2,4-triazine followed by oxidative aromatization of the dihydroadducts **3'a–d**. We found that the previously described conditions for the reaction of 1,2,4-triazines with 5,7-dimethoxycoumarins, namely reaction in the presence of 3 eq. methanesulfonic acid (MsOH) in acetic acid at ambient temperature for 24 h, can not be successfully used for the synthetic approach described herein. In contrast to our previous work, 3 equiv. methanesulfonic acid were not sufficient to efficiently catalyze this reaction, and a mixture of the starting coumarin **1** and triazine **2** was isolated from the reaction mixture. We found that increasing the amount of methanesulfonic acid to 10 equiv. allowed carrying out this first step with high yield. Subsequent oxidation of the formed dihydrotriazines was performed under the action of DDQ in 1,2-dichloroethane (DCE) with reflux, resulting in fully oxidized triazine derivatives with coumarins **3a–d** with good yields (65–77%) (Scheme 2).

It is well known that 1,2,4-triazines form pyridines under conditions of inverse electron-demand Diels-Alder reaction with norbornadiene. In the present work, the transformation of 1,2,4-triazines **3a–d** into 8-(bipyridyl)coumarins **4a–d** was carried out under autogenous pressure conditions according to the procedure from [33, 34]. The products of reaction **4a–d** were isolated in good yields. In addition, we would like to note that the reaction of 8-(bipyridyl)coumarins could not be carried out under reflux in 1,2-dichlorobenzene.



Scheme 2 The resulting products of coumarins and azines **3a–d** and **4a–d**.

The structures of compounds **3a-d** and **4a-d** were in accordance with ^1H NMR spectroscopy data. The characteristic signals of hydrogen at C-6 carbon atom in the triazine core in the region from 6.15 to 6.24 ppm were registered for the obtained compounds **3a-d**. In the case of conjugates **4a-d** the signal of the H-3 pyridine doublet in the region of 7.8–7.9 ppm with the constant $^1J = 8.0$ Hz was detected.

In addition, to confirm the structure of the obtained compounds **4a-d**, we carried out X-ray diffraction analysis. The obtained data of X-ray diffraction analysis on the example of compound **4b** unambiguously confirm the transformation of the 3-pyridyl-1,2,4-triazine moiety to the 2,2'-bipyridyl one (Figure 2).

3.2. Photophysical properties

The primary photophysical characteristics of compounds of the series 8-([2,2'-bipyridine]-6-yl)-5,7-dimethoxy-2H-chromen-2-ones **4a**, **4b**, **4c**, **4d** were studied. The results obtained are collected in Table 1. These compounds were found to exhibit fluorescence in acetonitrile solutions, with emission maxima in the range of 401–410 nm and fluorescence quantum yields up to 15%. An increase in the quantum yield value can be observed, in the presence of a methyl group at the C4 position of the coumarin core. As for compound **4a** containing a phenyl substituent in this position, its fluorescence is much weaker than that of the other compounds of this series. This phenomenon was previously described for 4-phenyl-substituted coumarins **4e**, **4q** containing monopyridyl substituents in position C-8 [35]. It is also worth noting that the values of Stokes shift of the considered series of compounds are quite high, reaching 114 nm, which is twice as high as for the previously published 5-phenyl- and 5-tolyl-2,2'-bipyridines [37], but is comparable to the Stokes shift of a number of coumarin-substituted (bi)pyridines (Table 1).

Thus, in the absorption spectra in acetonitrile solutions, the newly obtained coumarin-bipyridines **4a-d** exhibit intense absorption in the region of 212–296 nm, which corresponds to π - π^* transitions. Surprisingly, the substituted coumarin-bipyridine derivatives **4a-c**, in the case where $R^2 = H$, have quantum yields ranging from less than 0.1%, 5.6%, to 8.4%. On the other hand, it is noticeable that in compound **4d**, where $R^1 = \text{Me}$, $R^2 = \text{Bn}$, the emission maximum reaches 410 nm with a quantum yield value of 15.0%.

In our previous work [34], B3LYP/6-31G DFT calculations of the molecular structure of a representative compound containing a 4-methyl group in the coumarin ring and its 4-phenyl analog were carried out. The calculations showed that the 4-phenyl derivatives are characterized by the removal of the 5-methoxy group from the plane of the coumarin ring. Because of these structural features, effective conjugation in 4-phenyl derivatives is not possible, and the double bonds behave as isolated fluorophores, resulting in low fluorescence yields.

Obviously, the addition of pyridyl ring to 8-pyridyl coumarins at the C2' position gives rise to a potential coordination center. In the course of studying the complexation properties of compounds of the series of coumarin-substituted 2,2'-bipyridines it was found that titration of acetonitrile solutions of compounds **4a**, **4b**, **4c**, **4d** with AlCl_3 solution in THF in all cases is accompanied by a significant increase in the emission intensity (Figure 3), and in the case of the ligand **4a** a bathochromic shift of the emission maximum of the complex relative to the ligand by 67 nm is also observed (Figure 3–6).

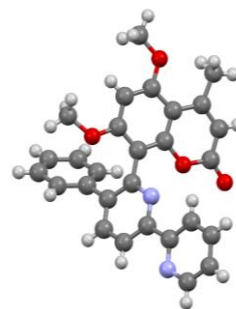


Figure 2 Structure of compound **4b** (CCDC2304245) obtained by X-ray diffraction.

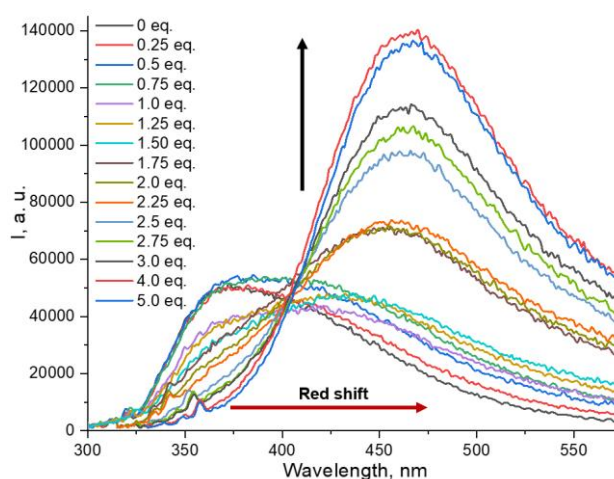


Figure 3 Solution emission spectra of compound **4a** upon addition of different concentrations of AlCl_3 solutions in THF.

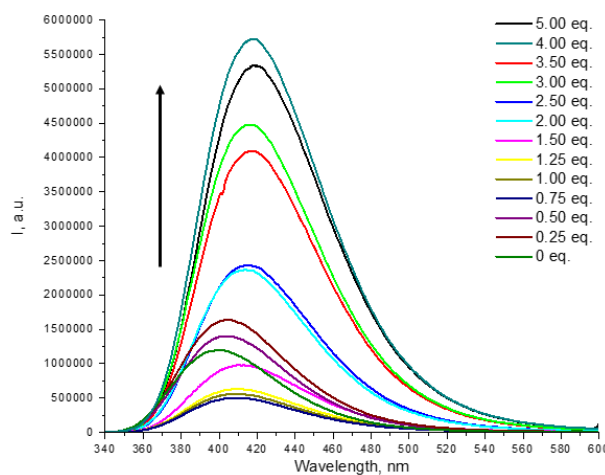
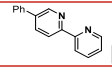
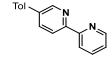
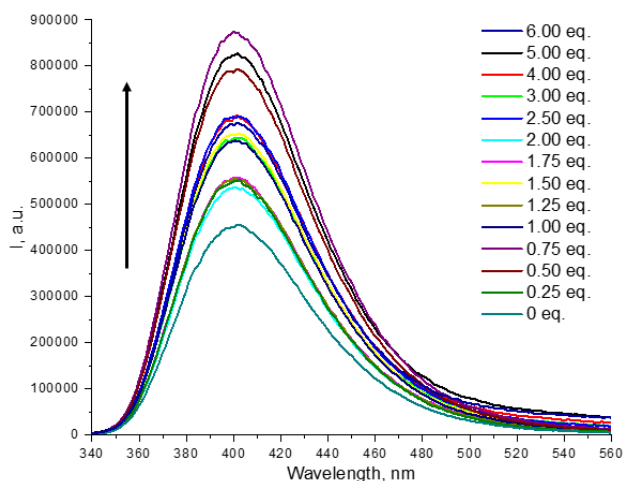
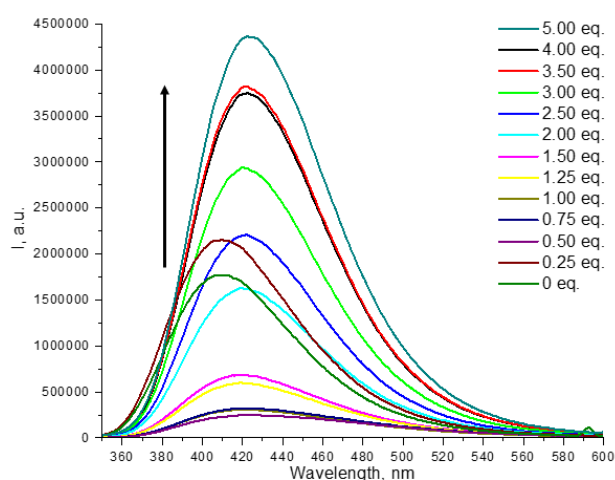


Figure 4 Solution emission spectra of compound **4b** upon addition of different concentrations of AlCl_3 solutions in THF.

Table 1 Photophysical characteristics of coumarins **4a**, **4b**, **4c**, **4d** and their previously described analogs.

	R ¹	R ²	R ³	X	λ_{abs} , nm ^a	λ_{em} , nm ^b	$\Delta\lambda$, nm	Φ , % ^c
4a	Ph	H	Tol	N	238, 292	408	116	<0.1
4b	Me	H	Ph	N	227, 294	401	107	5.6
4c	Me	H	Tol	N	212, 237, 296	401	105	8.4
4d	Me	Bn	Tol	N	241, 296	410	114	15.0
4e [34]	Me	H	Tol	CH	212, 260, 300	402	102	14.4
4q [34]	Me	Bn	Tol	CH	211, 252, 296–300	101	110	13.3
 [37]	-	-	Ph	N	298	357	59	3.2
 [37]	-	-	Tol	N	302	360	58	17.0

^a Maximum of absorption in acetonitrile at room temperature; ^b maximum of emission in acetonitrile at room temperature; ^c quantum yield measured by absolute method in acetonitrile solution at room temperature

**Figure 5** Solution emission spectra of compound **4c** upon addition of different concentrations of AlCl_3 solutions in THF.**Figure 6** Solution emission spectra of compound **4d** upon addition of different concentrations of AlCl_3 solutions in THF.

In the case of titration of compounds **4a–d** with Zn^{2+} and Cd^{2+} ions, a significant increase in the emission intensity and bathochromic shifts of the emission maximum of the

complexes relative to the ligands were also observed (see supplementary materials).

The opposite situation is observed when titrating acetonitrile solutions of ligands **4a**, **4b**, **4c**, **4d** with CuCl_2 solution in THF (Figures 7–10). Here, an increase in the concentration of Cu^{2+} cations in the analyzed solutions is accompanied by a sharp drop in the emission intensity up to the complete loss of fluorescence properties.

Further, the solvatochromic properties of the compounds and their complexes with Al^{3+} in various organic solvents were investigated at a concentration of $1.33 \cdot 10^{-5} \text{ M}^{-1}$. Based on the results of a series of experiments, positive solvatochromism was found for coumarins **4a**, **4b**, **4c** as well as their complexes with Al^{3+} . The obtained emission spectra of the compounds and complexes are shown in Figures 11–12 (other spectra are presented in the supplementary materials).

The difference of dipole moments of the ground and excited states in Debye units was calculated for the samples based on the graphical dependence of the Stokes shift difference on the orientational polarizability of the solvents in accordance with the Lippert-Mataga equation [38–42] (Figure 13).

Based on the calculated $\Delta\mu$ values (Table 2), it can be concluded that the most pronounced solvatochromic properties are possessed by ligand **4a** (14.89 D). At the same time, it should be noted that, based on the data found, in the case of compound **4c** there is a 1.5-fold enhancement of solvatochromic properties in the process of complexation with Al^{3+} . No solvatochromic properties were detected for compound **4d**.

Finally, to confirm the phenomenon of positive solvatochromism of the considered compounds and their complexes with Al^{3+} , we analyzed the dependence of the bathochromic shifts of the emission maxima on the quantitative criteria of the polarity of the solvents used, in particular, according to the Kosower diagrams [43–47].

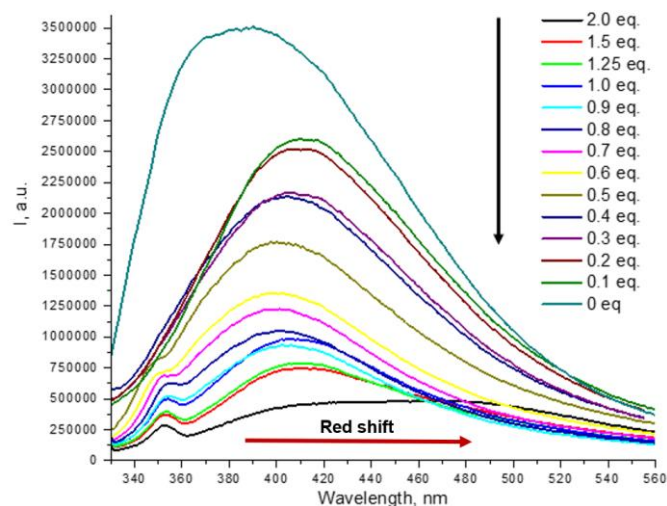


Figure 7 Solution emission spectra of compound **4a** upon addition of different concentrations of CuCl_2 solutions in THF.

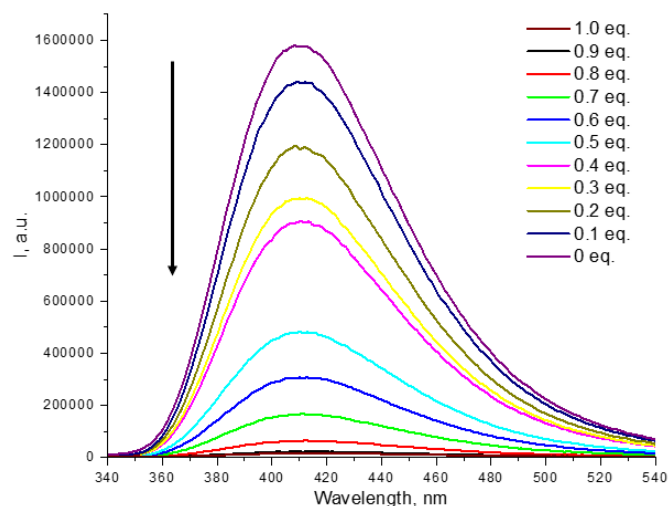


Figure 10 Solution emission spectra of compound **4d** upon addition of different concentrations of CuCl_2 solutions in THF.

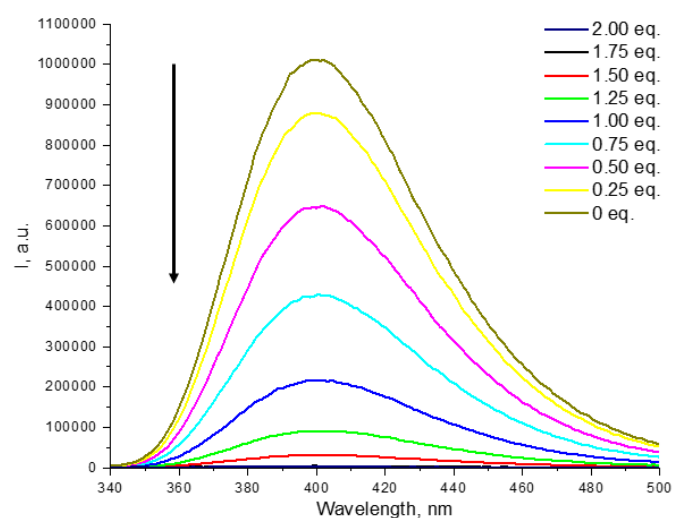


Figure 8 Solution emission spectra of compound **4b** upon addition of different concentrations of CuCl_2 solutions in THF.

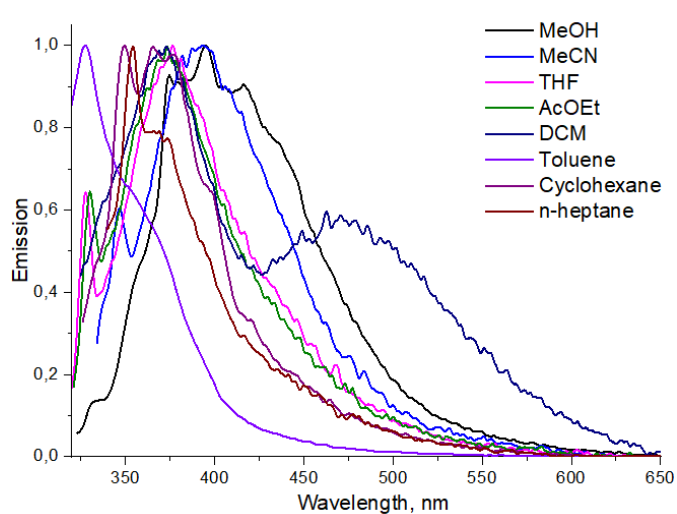


Figure 11 Emission spectra of compound **4a** in various solvents.

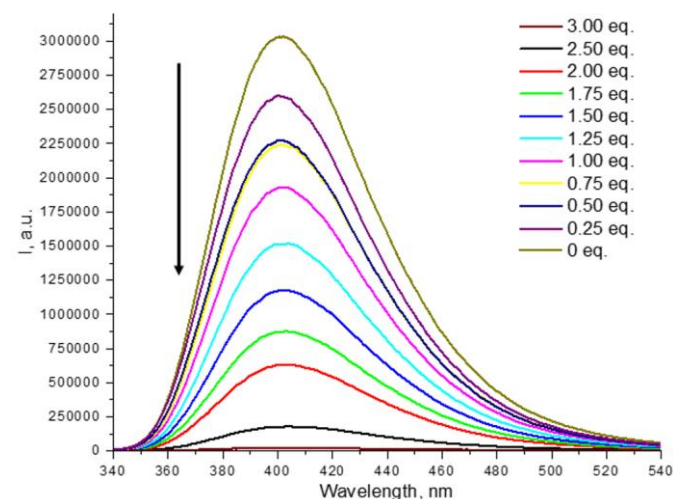


Figure 9 Solution emission spectra of compound **4c** upon addition of different concentrations of CuCl_2 solutions in THF.

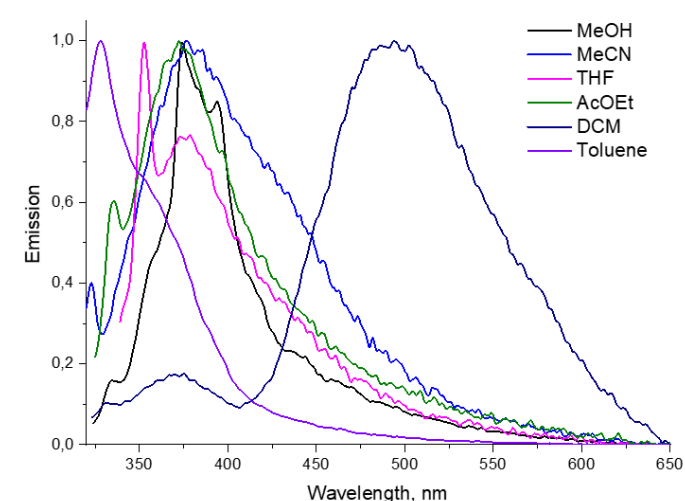


Figure 12 Emission spectra of compound **4a** with Al^{3+} in various solvents.

Table 2 Calculation data for the difference between the dipole moments of the ground and excited state switching of compounds **4a**, **4b**, **4c** and their complexes with Al³⁺.

Compound/Complex	Increment	R ²	Δμ, D
4a	17455	0.90	14.89
4a +Al ³⁺	14822	0.98	13.75
4b	6663	0.91	9.20
4b +Al ³⁺	7101	0.91	9.50
4c	9353	0.98	10.90
4c +Al ³⁺	22124	0.94	16.77

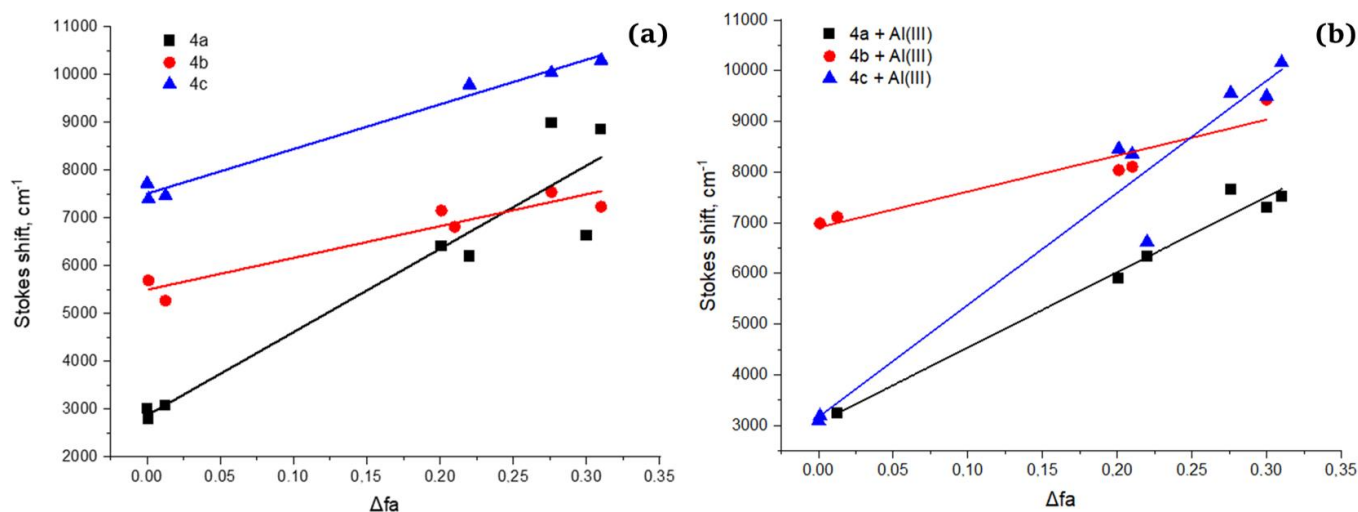
The results obtained in almost all cases correlate well with the quantitative values of the polarity of the corresponding solvents. However, an exception was observed in the case of DMSO for complexes **4a** and **4b**, as well as the latter ligand, where the emission maxima in this solvent slightly exceed that in the acetonitrile solution (Table 3, entry 3). However, considering the close values of the polarity criteria of DMSO and acetonitrile within both scales (71.1 and 71.3 kcal/mol by Kosover or 45.1 and 45.6 kcal/mol by Dimroth/Reichardt, respectively), these deviations can be considered insignificant. A more significant, but also not crucial, deviation from the regularities was noted for compound **4a** in the case of toluene (Table 3, entry 6), where the value of the wavelength of the main emission maximum is significantly lower compared to cyclohexane and n-heptane, despite very close values of the polarity criteria.

4. Limitation

In this paper, a convenient method for the synthesis of 8-[2,2'-bipyridinyl]coumarins starting from 1,2,4-triazinyl coumarins by a three-step reaction was proposed. In addition, the primary photophysical properties, the influence of solvent polarity, and the reliability of experimental results with mathematical calculations using the Lippert-Mataga equation and Kosower diagram were investigated. However, the analyte determination concentrations and some differences in photophysical characteristics have not been fully determined in this work. In further in-depth studies, we will try to explore additional photophysical compounds, expand the application to other analytes, and achieve the desired photophysical properties.

5. Conclusions

Thus, the work resulted in a convenient, simple and efficient route to synthesizing coumarin-bipyridine conjugates. This approach was characterized by easy availability of starting reagents, refusal of reaction catalysis by metals, and good yields. In addition, primary results on the photophysical properties of coumarin-bipyridines, the influence of solvent polarity, and the change of properties upon titration with Al³⁺, Cu²⁺, Zn²⁺, Cd²⁺ ions were found. The discovered optical properties of the obtained complexes of coumarin-bipyridines with metals open up possibilities for obtaining new efficient chemosensors.

**Figure 13** Graphical dependences of the Stokes shift difference on the orientational polarizability of solvents for ligands **4a**, **4b**, **4c** (a) and their complexes with Al³⁺ (b).**Table 3** Solvatochromic properties of compounds **4a**, **4b**, and **4c** and their complexes with Al³⁺.

	MeOH	MeCN	DMSO	DCM	THF	Toluene	n-Heptane	Cyclohexane
Z, kcal/mol	83.6	71.3	71.1	64.7	58.8			
E _T , kcal/mol	55.4	45.6	45.1	40.7	37.4	33.9	31.1	30.9
4a	416	395	407	373	-	328	354	349
4a +Al ³⁺	394	376	386	375	-	352	-	-
4b	458	-	408	-	385	382	-	372
4b +Al ³⁺	-	403	-	-	386	383	370	-
4c	449	-	450	403	-	385	377	374
4c +Al ³⁺	459	404	407	398	388	-	370	370

● Supplementary materials

This manuscript contains supplementary materials, which are available on the corresponding online page.

● Funding

The research was carried out within the framework of the Strategic Academic Leadership Program "Priority-2030" under Measure T, procurement No. PRTS48C4T28.2-23 "Payment of grants for scientific research of the University's research staff", on the topic "Fluorophores based on coumarin framework: synthesis and photophysical properties".

● Acknowledgments

The research funding from the Ministry of Science and Higher Education of the Russian Federation (Ural Federal University Program of Development within the Priority-2030 Program) is gratefully acknowledged.

● Author contributions

Conceptualization: A.D.S.

Data curation: A.D.S.

Formal Analysis: R.F.F., Y.K.S., A.P.P.

Funding acquisition: A.D.S.

Investigation: A.P.P., P.A.S.

Methodology: A.D.S., I.A.K., D.S.K.

Project administration: R.F.F.

Resources: A.D.S., A.P.P., D.S.K.

Software: A.D.S., P.A.S.

Supervision: I.A.K.

Validation: I.L.N., D.S.K., Y.K.S.

Visualization: I.L.N.

Writing original draft: A.D.S., I.A.K.

Writing review & editing: A.D.S., R.F.F., I.A.K.

● Conflict of interest

The authors declare no conflict of interest.

● Additional information

Author IDs:

Ramil F. Fatykhov, Scopus ID [57190761230](https://scopus.com/authid/detail.url?authorID=57190761230);

Igor A. Khalymbadzha, Scopus ID [18434200300](https://scopus.com/authid/detail.url?authorID=18434200300);

Ainur D. Sharapov, Scopus ID [57201740165](https://scopus.com/authid/detail.url?authorID=57201740165);

Anastasia P. Potapova, Scopus ID [57463666800](https://scopus.com/authid/detail.url?authorID=57463666800);

Dmitry S. Kopchuk, Scopus ID [14123383900](https://scopus.com/authid/detail.url?authorID=14123383900);

Igor L. Nikonov, Scopus ID [55910292900](https://scopus.com/authid/detail.url?authorID=55910292900);

Yaroslav K. Shtaitz, Scopus ID [57201778255](https://scopus.com/authid/detail.url?authorID=57201778255);

Pavel A. Slepukhin, Scopus ID [6506482417](https://scopus.com/authid/detail.url?authorID=6506482417).

Websites:

Ural Federal University, <https://urfu.ru/en>;

Institute of Organic Synthesis, <https://iosuran.ru>;

Ural State Forest Engineering University,
<http://usfeu.ru/>.

References

- Cao D, Liu Z, Verwilt P, Koo S, Jangjili P, Kim JS, Lin W. Coumarin-Based Small-Molecule Fluorescent Chemosensors. *Chemical Reviews*. 2019;119(18):10403–10519. doi:[10.1021/acs.chemrev.9b00145](https://doi.org/10.1021/acs.chemrev.9b00145)
- Górski K, Deperasińska I, Baryshnikov GV, Ozaki S, Kamada K, Ågren H, Gryko DT. Quadrupolar dyes based on highly polarized coumarins. *Org Lett*. 2021;23(17):6770–6774. doi:[10.1021/acs.orglett.1c02349](https://doi.org/10.1021/acs.orglett.1c02349)
- Shaydyuk YO, Bashmakova NV, Klishevich GV, Dmytruk AM, Kachkovsky OD, Kuziv IB, Dubey IY, Belfield KD, Bondar MV. Nature of linear spectral properties and fast relaxations in the excited states and two-photon absorption efficiency of 3-thiazolyl and 3-phenylthiazolyl coumarin derivatives. *ACS Omega*. 2023;8(12):11564–11573. doi:[10.1021/acsomega.3c00654](https://doi.org/10.1021/acsomega.3c00654)
- Verma P, Pal, H. Aggregation Studies of Dipolar Coumarin-153 Dye in Polar Solvents: A Photophysical Study. *J Phys Chem A*. 2014;118(34):6950–6964. doi:[10.1021/jp506138w](https://doi.org/10.1021/jp506138w)
- Jana K, Sarkar D, Jaiswal P, Moorthy JN. Synthesis and Excited-State Properties of Donor–Acceptor Azahelical Coumarins. *J Org Chem*. 2023;88(11):6611–6622. doi:[10.1021/acs.joc.2c02810](https://doi.org/10.1021/acs.joc.2c02810)
- Xu Z, Chen X, Kim HN, Yoon J. Sensors for the optical detection of cyanide ion. *Chem Soc Rev*. 2010;39:127–137. doi:[10.1039/B907368J](https://doi.org/10.1039/B907368J)
- Zhou Y, Zhang JF, Yoon J. Fluorescence and colorimetric chemosensors for fluoride-ion detection. *Chem Rev*. 2014;114:5511–5571. doi:[10.1021/cr400352m](https://doi.org/10.1021/cr400352m)
- Kim SK, Lee DH, Hong JI, Yoon J. Chemosensors for pyrophosphate. *Acc Chem Res*. 2009;42:23–31. doi:[10.1021/ar800003f](https://doi.org/10.1021/ar800003f)
- Wu J, Kwon B, Liu W, Anslyn EV, Wang P, Kim JS. Chromogenic/fluorogenic ensemble chemosensing systems. *Chem Rev*. 2015;115:7893–7843. doi:[10.1021/cr500553d](https://doi.org/10.1021/cr500553d)
- Hargrove AE, Nieto S, Zhang T, Sessler JL, Anslyn EV. Artificial receptors for the recognition of phosphorylated molecules. *Chem Rev*. 2011;111:6603–6782. doi:[10.1021/cr100242s](https://doi.org/10.1021/cr100242s)
- Shiraishi Y, Nakamura M, Hayashi N, Hirai T. Coumarin-spiropyran dyad with a hydrogenated pyran moiety for rapid, selective, and sensitive fluorometric detection of cyanide anion. *Anal Chem*. 2016;88:6805–6811. doi:[10.1021/acs.analchem.6b01279](https://doi.org/10.1021/acs.analchem.6b01279)
- Que EL, Domaille DW, Chang CJ. Metals in neurobiology: probing their chemistry and biology with molecular imaging. *Chem Rev*. 2008;108:1517–1549. doi:[10.1021/cro78203u](https://doi.org/10.1021/cro78203u)
- Verwilt P, Sunwoo K, Kim JS. The role of copper ions in pathophysiology and fluorescent sensors for the detection thereof. *Chem Commun*. 2015;51:5556–5571. doi:[10.1039/C4CC10366A](https://doi.org/10.1039/C4CC10366A)
- Chen X, Pradhan T, Wang F, Kim JS, Yoon J. Fluorescent chemosensors based on spiroring-opening of xanthenes and related derivatives. *Chem Rev*. 2012;112:1910–1956. doi:[10.1021/cr200201z](https://doi.org/10.1021/cr200201z)
- Zhang JF, Zhou Y, Yoon J, Kim JS. Recent progress in fluorescent and colorimetric chemosensors for detection of precious metal ions (silver, gold and platinum ions). *Chem Soc Rev*. 2011;40:3416–3429. doi:[10.1039/c1cs15028f](https://doi.org/10.1039/c1cs15028f)
- Qian X, Xu Z. Fluorescence imaging of metal ions implicated in diseases. *Chem Soc Rev*. 2015;44:4487–4493. doi:[10.1039/C4CS00292J](https://doi.org/10.1039/C4CS00292J)
- Sun W, Guo S, Hu C, Fan J, Peng X. Recent development of chemosensors based on cyanine platforms. *Chem Rev*. 2016;116:7768–7817. doi:[10.1021/acs.chemrev.6b00001](https://doi.org/10.1021/acs.chemrev.6b00001)
- Dong B, Song X, Kong X, Wang C, Tang Y, Liu Y, Lin W. Simultaneous near-infrared and two-photon in vivo imaging of H₂O₂ using a ratiometric fluorescent probe based on the

- unique oxidative rearrangement of oxonium. *Adv Mater.* 2016;28:8755–8759. doi:[10.1002/adma.201602939](https://doi.org/10.1002/adma.201602939)
19. Men Y, Li Z, Zhang J, Tong Z, Xi Z, Qiu X, Yi L. Rational design and synthesis of fast-response NBD-based fluorescent probes for biothiols. *Tetrahedron Lett.* 2015;56:5781–5786. doi:[10.1016/j.tetlet.2015.08.073](https://doi.org/10.1016/j.tetlet.2015.08.073)
20. He L, Yang X, Xu K, Yang Y, Lin W. A multifunctional logic gate by means of a triple-chromophore fluorescent biothiol probe with diverse fluorescence signal patterns. *Chem Commun.* 2017;53:13168–13171. doi:[10.1039/C7CC07296A](https://doi.org/10.1039/C7CC07296A)
21. Manjare ST, Kim Y, Churchill DG. Selenium- and tellurium-containing fluorescent molecular probes for the detection of biologically important analytes. *Acc Chem Res.* 2014;47:2985–2998. doi:[10.1021/ar500187v](https://doi.org/10.1021/ar500187v)
22. Dong B, Zheng K, Tang Y, Lin W. Development of green to near-infrared turn-on fluorescent probes for the multicolour imaging of nitroxyl in living systems. *J Mater Chem B.* 2016;4:1263–1269. doi:[10.1039/C5TB02073E](https://doi.org/10.1039/C5TB02073E)
23. Zhang Q, Zhu Z, Zheng Y, Cheng J, Zhang N, Long Y-T, Zheng J, Qian X, Yang Y. A three-channel fluorescent probe that distinguishes peroxynitrite from hypochlorite. *J Am Chem Soc.* 2012;134:18479–18482. doi:[10.1021/ja305046u](https://doi.org/10.1021/ja305046u)
24. Signore G, Nifosi R, Albertazzi L, Storti B, Bizzarri R. Polarity-sensitive coumarins tailored to live cell imaging. *J Am Chem Soc.* 2010;132:1276–1288. doi:[10.1021/ja9050444](https://doi.org/10.1021/ja9050444)
25. Hirosawa S, Arai S, Takeoka S. A TEMPO-conjugated fluorescent probe for monitoring mitochondrial redox reactions. *Chem Commun.* 2012;48:4845–4847. doi:[10.1039/c2cc30603d](https://doi.org/10.1039/c2cc30603d)
26. Xiao-ya S, Teng L, Jie S, Xiao-jing W. Synthesis and application of coumarin fluorescence probes. *RSC Adv.* 2020;10:10826–10847. doi:[10.1039/C9RA10290F](https://doi.org/10.1039/C9RA10290F)
27. Li T, Fang R, Wang B, Shao Y, Liu J, Zhang S, Yang Z. A simple coumarin as a turn-on fluorescence sensor for Al(III) ions. *Dalton Trans.* 2014;43:2741–2743. doi:[10.1039/C3DT52414K](https://doi.org/10.1039/C3DT52414K)
28. Guha S, Lohar S, Sahana A, Banerjee A, Safin DA, Babashkina MG, Mitoraj MP, Bolte M, Garcia Y, Mukhopadhyay SK, Das D. A coumarin-based “turn-on” fluorescent sensor for the determination of Al³⁺: single crystal X-ray structure and cell staining properties. *Dalton Trans.* 2013;42:10198–10207. doi:[10.1039/c3dt51045j](https://doi.org/10.1039/c3dt51045j)
29. García-Beltrán O, Cassels BK, Mena N, Nuñez MT, Yañez O, Caballero J. A coumarinylaldoxime as a specific sensor for Cu²⁺ and its biological application. *Tetrahedron Lett.* 2014;55:873–876. doi:[10.1016/j.tetlet.2013.12.033](https://doi.org/10.1016/j.tetlet.2013.12.033)
30. Kumari C, Sain D, Kumar A, Debnath S, Saha P, Dey S. Intracellular detection of hazardous Cd²⁺ through a fluorescence imaging technique by using a nontoxic coumarin based sensor. *Dalton Trans.* 2017;46:2524–2531. doi:[10.1039/C6DT04833A](https://doi.org/10.1039/C6DT04833A)
31. Maity D, Govindaraju T. A differentially selective sensor with fluorescence turn-on response to Zn²⁺ and dual-mode ratiometric response to Al³⁺ in aqueous media. *Chem Commun.* 2012;48:1039–1041. doi:[10.1039/C1CC16064](https://doi.org/10.1039/C1CC16064)
32. Fatykhov RF, Khalymbadza IA, Sharapov AD, Potapova AP, Starnovskaya ES, Kopchuk DS, Chupakhin, ON. Expedient synthesis of 1,2,4-triazinyl substituted benzo[c]coumarins via double oxidation strategy. *Chim Tech Acta.* 2023;10(2):202310205. doi:[10.15826/chimtech.2023.10.2.05](https://doi.org/10.15826/chimtech.2023.10.2.05)
33. Fatykhov RF, Savchuk MI, Starnovskaya ES, Bobkina MV, Kopchuk DS, Nosova EV, Zyryanov GV, Khalymbadza IA, Chupakhin ON, Charushin VN, Kartsev, VG. Nucleophilic substitution of hydrogen—the Boger reaction sequence as an approach towards 8-(pyridin-2-yl)coumarins. *Mendeleev Commun.* 2019;29(3):299–300. doi:[10.1016/j.mencom.2019.05.019](https://doi.org/10.1016/j.mencom.2019.05.019)
34. Fatykhov RF, Sharapov AD, Starnovskaya ES, Shtaitz, YK, Savchuk MI, Kopchuk DS, Nikonov IL, Zyryanov GV, Khalymbadza IA, Chupakhin ON. Coumarin-pyridine push-pull fluorophores: Synthesis and photophysical studies. *Spectrochim Acta A Mol Biomol Spectros.* 2022;267:120499. doi:[10.1016/j.saa.2021.120499](https://doi.org/10.1016/j.saa.2021.120499)
35. Sharapov AD, Fatykhov RF, Khalymbadza IA, Sharutin VV, Santra S, Zyryanov G, Chupakhin ON, Ranu BC. Mechanochemical synthesis of coumarins via Pechmann condensation under solvent-free conditions: an easy access to coumarins and annulated pyrano[2,3-f] and [3,2-f]indoles. *Green Chem.* 2022;4(6):2429–2437. doi:[10.1039/d1gc04564d](https://doi.org/10.1039/d1gc04564d)
36. Santra S, Sharapov AD, Fatykhov RF, Potapova AP, Khalymbadza IA, Valieva MI, Kopchuk DS, Zyryanov GV, Bunev AS, Melekhin VV, Gaviko VS, Zonov AA. Xanthone-1,2,4-triazine and Acridone-1,2,4-triazine Conjugates: Synthesis and anticancer activity. *Pharmaceut.* 2023;16(3):403. doi:[10.3390/ph16030403](https://doi.org/10.3390/ph16030403)
37. Shabunina OV, Kopchuk DS, Ustinova MM, Kozhevnikov DN, Kozhevnikov VN, König B. Facile Synthesis Of 6-Aryl-3-Pyridyl-1,2,4-Triazines As A Key Step Toward Highly Fluorescent 5-Substituted Bipyridines And Their Zn(II) And Ru(II) Complexes. *Tetrahedron.* 2008;64(37):8963–8973. doi:[10.1016/j.tet.2008.06.040](https://doi.org/10.1016/j.tet.2008.06.040)
38. Lakowicz JR. Principles of Fluorescence Spectroscopy. Springer. Boston, 2006. 205–235 p.
39. Von Lippert EZ. Spektroskopische Bestimmung des Dipolmomentes aromatischer Verbindungen im ersten angeregten Singulettzustand. *Ber Bunsenges. Phys Chem.* 1957;61(8):962–975. doi:[10.1002/bbpc.19570610819](https://doi.org/10.1002/bbpc.19570610819)
40. Mataga N, Kaifu Y, Koizumi M. Solvent effects upon fluorescence spectra and the dipole moments of excited molecules. *Bull Chem Soc Jpn.* 1956;29:465–470. doi:[10.1246/BCSJ.29.465](https://doi.org/10.1246/BCSJ.29.465)
41. Kawski A. On the estimation of excited-state dipole moments from solvatochromic shifts of absorption and fluorescence spectra, *Z. Naturforsch A.* 2002;57(5):255–262. doi:[10.1515/zna-2002-0509](https://doi.org/10.1515/zna-2002-0509)
42. Rabek JF. Progress in photochemistry and photophysics, vol. V. CRC Press. Boca Raton, 2016. 1–208 p.
43. Kopchuk DS, Chepchugov NV, Starnovskaya ES, Khasanov AF, Krinochkin AP, Santra S, Zyryanov GV, Das P, Majee A, Rusinov VL, Charushin VN. Synthesis and optical properties of new 2-(5-arylpyridine-2-yl)-6-(het)arylquinoline-based “push-pull” fluorophores. *Dyes Pigm.* 2019;167:151–156. doi:[10.1016/j.dyepig.2019.04.029](https://doi.org/10.1016/j.dyepig.2019.04.029)
44. Kosower EM. An Introduction to Physical Organic Chemistry. Wiley. New York, 1968. 293 p.
45. Kosower EM, The Effect of Solvent on Spectra. I. A New Empirical Measure of Solvent Polarity: Z-Values. *J Am Chem Soc.* 1958;80(13):3253–3260. doi:[10.1021/ja01546a020](https://doi.org/10.1021/ja01546a020)
46. Dimroth K, Reichardt C, Siepmann T, Bohlmann F. Über Pyridinium-Nphenol-betaïne und ihre Verwendung zur Charakterisierung der Polarität von Lösungsmitteln, Liebigs. *Ann Chem.* 1963;661(1):1–37. doi:[10.1002/jlac.19636610102](https://doi.org/10.1002/jlac.19636610102)
47. Reichardt C. Über Pyridinium-N-phenol-betaïne und ihre Verwendung zur Charakterisierung der Polarität von Lösungsmitteln, VI. Erweiterung der Lösungsmittelpolaritätsskala durch Bestimmung neuer molarer Übergangsennergien (ET-Werte), Liebigs. *Ann Chem.* 1971;752(1):64–67. doi:[10.1002/jlac.19717520109](https://doi.org/10.1002/jlac.19717520109)
48. Sheldrick GM. A short history of SHELX. *Acta Crystallogr.* 2008;A64:112–122. doi:[10.1107/S0108767307043930](https://doi.org/10.1107/S0108767307043930)
49. CrysAlisPro, version 1.171.39.38a, Data Collection, Reduction and Correction Program, Rigaku Oxford Diffraction, 2017.
50. Sharapov, AD, Fatykhov, RF, Khalymbadza, IA, Valieva, MI, Nikonov, IL, Taniya, OS, Kopchuk, DS, Zyryanov, GV, Potapova, AP, Novikov, AS, Sharutin, VV, Chupakhin, ON. Fluorescent Pyranoindole Congeners: Synthesis and Photophysical Properties of Pyrano[3,2-f], [2,3-g], [2,3-f], and [2,3-e]Indoles. *Molecules.* 2022;27(24):8867. doi:[10.3390/molecules27248867](https://doi.org/10.3390/molecules27248867)